

# Stark effect spectroscopy of *Rhodobacter sphaeroides* and *Rhodospseudomonas viridis* reaction centers

(photosynthesis/electron transfer/electroabsorption/electrochromism)

DAVID J. LOCKHART AND STEVEN G. BOXER

Department of Chemistry, Stanford University, Stanford, CA 94305

Communicated by Gerhard L. Closs, September 11, 1987 (received for review July 22, 1987)

**ABSTRACT** The nature of the initially excited state of the primary electron donor or special pair has been investigated by Stark effect spectroscopy for reaction centers from the photosynthetic bacteria *Rhodospseudomonas viridis* and *Rhodobacter sphaeroides* at 77 K. The data provide values for the magnitude of the difference in permanent dipole moment between the ground and excited state,  $|\Delta\mu|$ , and the angle  $\zeta$  between  $\Delta\mu$  and the transition dipole moment for the electronic transition.  $|\Delta\mu|$  and  $\zeta$  for the lowest-energy singlet electronic transition associated with the special pair primary electron donor were found to be very similar for the two species.  $|\Delta\mu|$  for this transition is substantially larger than for the  $Q_y$  transitions of the monomeric pigments in the reaction center or for pure monomeric bacteriochlorophylls, for which Stark data are also reported. We conclude that the excited state of the special pair has substantial charge-transfer character, and we suggest that charge separation in bacterial photosynthesis is initiated immediately upon photoexcitation of the special pair. Data for *Rhodobacter sphaeroides* between 340 and 1340 nm are presented and discussed in the context of the detection of charge-transfer states by Stark effect spectroscopy.

The recent elucidation of the organization of the reactive components in reaction centers (RCs) from photosynthetic bacteria by x-ray diffraction (1–4) makes possible an analysis of the initial charge-separation mechanism from first principles. The first step in such an analysis is the calculation of the spectroscopic properties of the RC from several species, including the absorption, circular dichroism, and linear dichroism spectra (5–9). In a recent report we demonstrated that a quantitative analysis of the effect of an electric field on the absorption spectrum (the Stark effect spectrum) in *Rhodobacter sphaeroides* RCs at room temperature provides additional observables for comparison with theory (10). This work followed up on an earlier preliminary report by deLeeuw *et al.* (11). In the present communication we extend these measurements to a different species, *Rhodospseudomonas viridis*, and to low temperatures (12).

Quantitative analysis of the Stark effect spectrum provides information on the magnitude of the difference in permanent dipole moment between the ground and excited state,  $|\Delta\mu|$ , and on the angle,  $\zeta$ , between  $\Delta\mu$  and the transition dipole moment. Since the orientation of the transition dipole moment can be determined relative to the molecular axes from single-crystal polarized absorption measurements, the angle  $\zeta$  can be related to the movement of charge associated with excitation of the chromophores in the RC. Stark effect data have also been obtained for monomeric photosynthetic chromophores, and this information should be useful for testing the reliability of the

wave functions that are used for the calculation of RC spectral properties and electron transfer pathways.

## EXPERIMENTAL

*Rps. viridis* RCs were prepared as previously described for *Rb. sphaeroides* (13), except that a sucrose density gradient centrifugation replaced the second extraction with lauryldimethylamine oxide/5 mM Tris-HCl, pH 8.0, were embedded in poly(vinyl alcohol) (PVA) films, which were then coated with semitransparent nickel electrodes as described earlier for *Rb. sphaeroides* RCs (10). Bacteriochlorophylls *a* and *b* (BChl *a* and *b*) and bacteriopheophytins *a* and *b* (BPheo *a* and *b*) were prepared by standard methods (14) and were judged to be pure by their electronic absorption spectra and thin-layer chromatography. The chromophores were embedded in films of poly(methyl methacrylate) (PMMA), which were coated with nickel electrodes.

Stark spectra were obtained with the apparatus described previously (10). Spectra at 77 K were obtained with the samples immersed directly in liquid nitrogen. For measurements of  $\zeta$  the probing light was horizontally polarized and the angle,  $\chi$ , between the electric vector of the light and the applied field direction was varied by rotating the sample about a vertical axis (see figure 1 of ref. 10 for further details). A cooled germanium detector was used between 1000 and 1400 nm.

## RESULTS

The Stark spectrum of *Rps. viridis* RCs in a PVA film at 77 K is shown in Fig. 1 for the lowest-energy singlet electronic transitions of the chromophores ( $Q_y$  region). Data at 77 K for the comparable region in *Rb. sphaeroides* RCs are shown in Fig. 2. No feature whose  $\Delta A$  is greater than 1% of that observed at 874 nm was observed between 1000 and 1340 nm for *Rb. sphaeroides* RCs. The Stark spectrum in the  $Q_x$  and Soret regions for *Rb. sphaeroides* is shown in Fig. 3. The dependence of the magnitude of the Stark effect signal on the angle  $\chi$  for the  $Q_y$  transitions of the special pair in *Rps. viridis* and *Rb. sphaeroides* RCs and for six-coordinate BChl *a* and *b* is shown in Fig. 4. The dependence on  $\chi$  of the entire Stark spectrum in the  $Q_y$  region for both species is shown in Fig. 5.

Quantitative analysis of the Stark effect data was performed by using the methods described in ref. 10, which closely follow the earlier theoretical development of Liptay (15) and Mathies and Stryer (16). The change in absorption upon application of an electric field,  $\Delta A$ , due to a difference in permanent dipole moment between the ground state and the excited state to which the transition occurs for a randomly

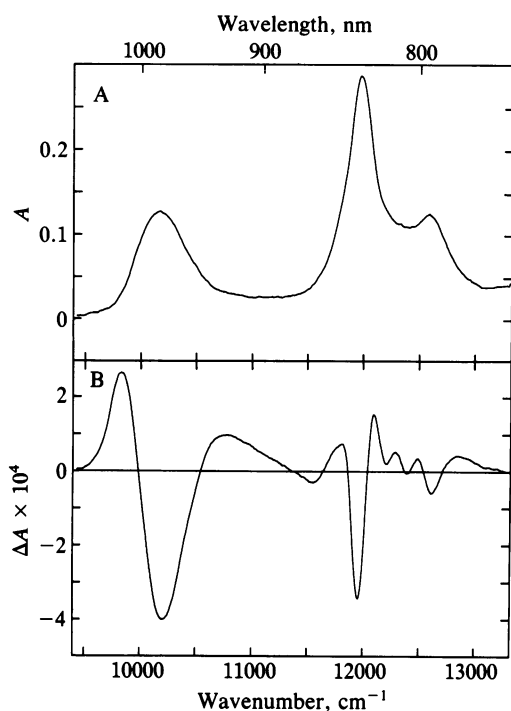


FIG. 1. Absorption (A) and Stark effect (B) spectra for *Rps. viridis* RCs in a PVA film in the  $Q_y$  region at 77 K ( $F_{\text{ext}} = 3.14 \times 10^5$  V/cm).

oriented immobilized sample is given by

$$\Delta A(\nu) = \frac{C_x}{30 h^2} F_{\text{int}}^2 \nu \frac{d^2(A/\nu)}{d\nu^2}, \quad [1]$$

where  $C_x = 5 \Delta\mu^2 + (3 \cos^2\chi - 1)[3(\mathbf{p} \cdot \Delta\mu)^2 - \Delta\mu^2]$ ,  $\chi$  is the

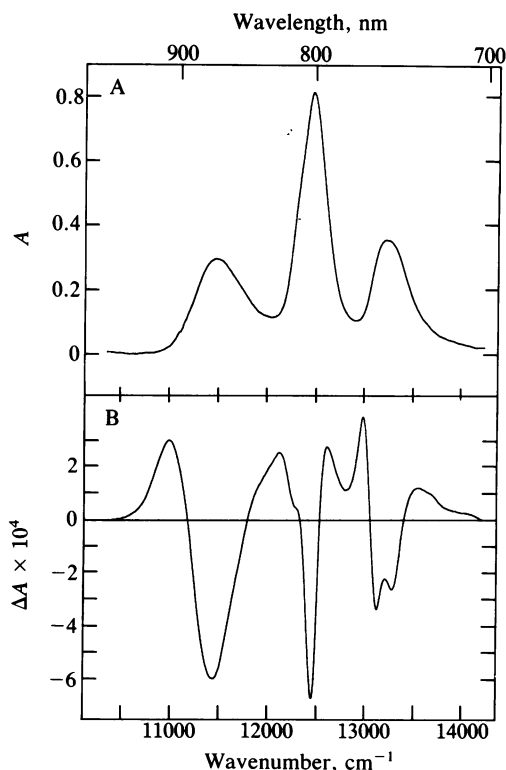


FIG. 2. Absorption (A) and Stark effect (B) spectra for *Rb. sphaeroides* RCs in a PVA film in the  $Q_y$  region at 77 K ( $F_{\text{ext}} = 2.59 \times 10^5$  V/cm).

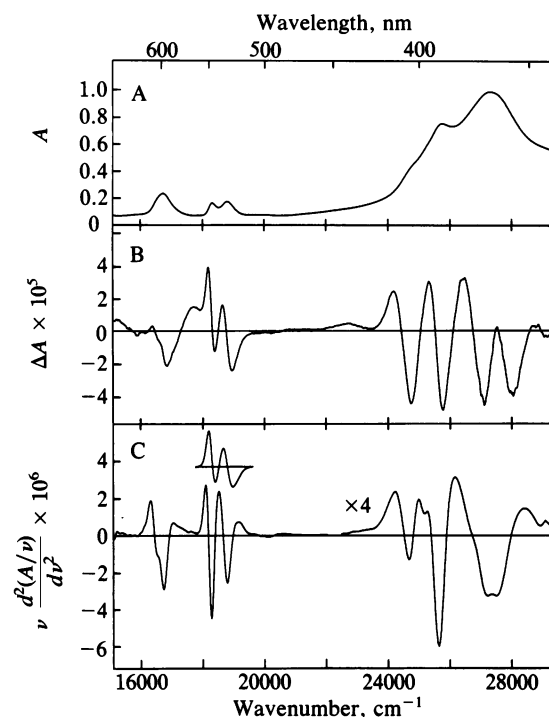


FIG. 3. Absorption (A), Stark effect (B), and second-derivative (C) spectra for the  $Q_x$  and Soret region of *Rb. sphaeroides* RCs at 77 K. The Stark effect spectrum was recorded with  $F_{\text{ext}} = 4.43 \times 10^5$  V/cm; the spectrum has been scaled (Eq. 1) to  $F_{\text{ext}} = 2.59 \times 10^5$  V/cm to facilitate comparison with the  $Q_y$  region (same sample as used for Fig. 2). (Inset) Appropriate first derivative (arbitrary units) of the monomeric BPheo  $a$   $Q_x$  absorption bands.

angle between the applied electric field direction and the polarization vector of the probing beam,  $h$  is Planck's constant, and  $\mathbf{p}$  is a unit vector in the direction of the transition dipole moment being probed at frequency  $\nu$ .  $F_{\text{int}}$  is the actual field felt by the molecules under investigation, which is different from the applied field because of the dielectric properties of the environment.  $F_{\text{int}}$  is related to the applied electric field,  $F_{\text{ext}}$ , by the local field correction:  $F_{\text{int}} =$

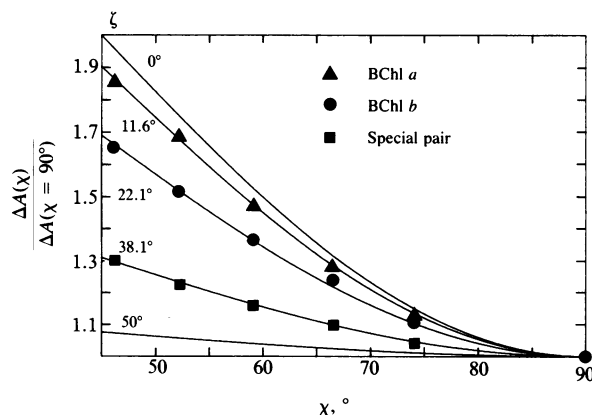


FIG. 4. Dependence of the experimental value of the change in absorption measured for the experimental angle  $\chi$  over the change in absorption for  $\chi = 90^\circ$  for the  $Q_y$  transition of the special pair in *Rps. viridis* and *Rb. sphaeroides* RCs (■; data for the two species are indistinguishable within the size of the symbols), for six-coordinate BChl  $b$  (●), and six-coordinate BChl  $a$  (▲) at 77 K. The solid lines are best fits of the data to the angle dependence in Eq. 1 for the values of the angle  $\zeta$  indicated on the left; theoretical curves are also included for  $\zeta = 0^\circ$  and  $50^\circ$  to indicate the sensitivity of the measurements to this angle.

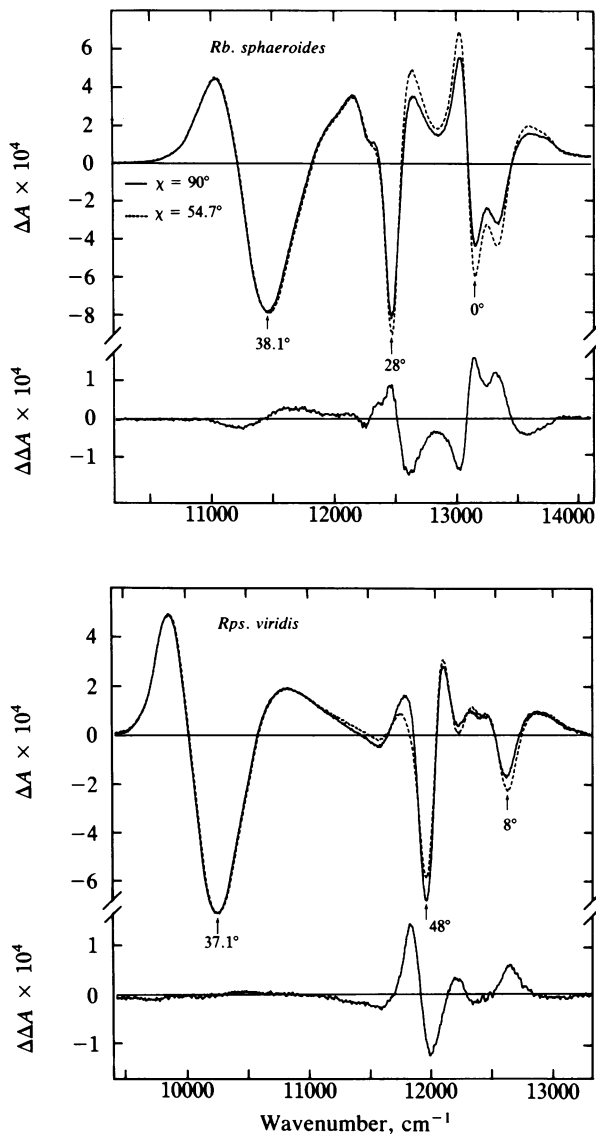


FIG. 5. Dependence of the Stark effect spectrum on the experimental angle  $\chi$  for the  $Q_y$  regions of *Rb. sphaeroides* ( $F_{\text{ext}} = 3.04 \times 10^5$  V/cm) and *Rps. viridis* ( $F_{\text{ext}} = 4.29 \times 10^5$  V/cm) RCs at 77 K. To facilitate comparison, the spectra in both panels have been normalized to make the value of the Stark signal equal at the minimum of the effect for the special pair (longest-wavelength) band. Data are shown at  $\chi = 90^\circ$  (solid lines) and  $\chi = 54.7^\circ$  (dotted lines), along with the difference ( $\Delta\Delta A$ ) for  $\chi = 90^\circ$  minus that for  $\chi = 54.7^\circ$  to accentuate variations in the values of  $\zeta$ . The values of  $\zeta$  measured at several energies are indicated below the vertical arrows.

$fF_{\text{ext}}$ . The value of  $f$  is typically on the order of 1.2–1.4 for a dielectric constant of 2, depending on the model used for the electrostatic field (10). We express the value of the dipole moment difference as the product of  $f^{-1}$  and the observed value of  $|\Delta\mu|$  assuming  $F_{\text{int}} = F_{\text{ext}}$  to clearly separate the experimental uncertainties from assumptions used to treat the local field.

The value of  $|\Delta\mu|$  was calculated from  $\nu[d^2(A/\nu)/d\nu^2]$ ,  $\zeta$  (Fig. 4), and  $\Delta A$  obtained near the peak of the absorption band, since the effect due to  $|\Delta\mu|$  is large and any polarizability (first-derivative) effects can be ignored. The application of Eq. 1 to obtain  $|\Delta\mu|$  is straightforward when the electronic transition is well resolved and has a simple absorption lineshape. This is not the case for the RC absorption spectrum; consequently a variety of approximate approaches have been used. For the pure monomeric chromophores in PMMA and for the monomeric BChl bands in

the RC,  $\nu[d^2(A/\nu)/d\nu^2]$  was determined by numerically differentiating the absorption spectrum. For the special pair  $Q_y$  absorption band the part of the band that does not overlap with other bands was fit to an exponential of a fourth-order polynomial function, which was numerically differentiated. Quantitative analysis of the data leads to the values summarized in Table 1.

## DISCUSSION

**Survey of Features in the Stark Spectrum.** At a qualitative level, it is apparent from the Stark effect spectra of both species that the dipole moment difference for the lowest energy band in the RC absorption spectrum, whose character is predominately determined by the dimeric primary electron donor or special pair, is much larger than for other features in the spectrum. The quantitative analysis summarized in Table 1 demonstrates that  $|\Delta\mu|$  for the  $Q_y$  transition of the special pair is likewise much larger than for pure BChl and that the values at both room temperature and 77 K are very similar for *Rps. viridis* and *Rb. sphaeroides* RCs. Furthermore, the angle  $\zeta$  between  $\Delta\mu$  and the transition dipole moment for the special pair  $Q_y$  transition is identical for both species within experimental error, but this angle differs from that determined for the monomeric chromophores. The remarkable similarity of both  $|\Delta\mu|$  and  $\zeta$  for the  $Q_y$  special pair absorption band of both species is consistent with the gross similarity of the special pair structures seen by x-ray diffraction (1–4). On the other hand, there is a significant chemical difference between BChl *a* and BChl *b*, and amino acids in the vicinity of the special pair are quite different for the two species (2). Apparently neither of these differences is sufficient to perturb the values of  $|\Delta\mu|$  or  $\zeta$ , both of which are expected to be very sensitive to variations in electronic structure.

For the purpose of discussion, we will use the conventional assignment of absorption bands to specific chromophores, recognizing that there is substantial electronic mixing. Because the absorption bands for the monomeric chromophores overlap substantially and one expects vibronic bands from the special pair in this region, it is difficult to quantitate  $|\Delta\mu|$  and  $\zeta$  for the monomer bands. For *Rb. sphaeroides*, the values of  $|\Delta\mu|$  for the partially resolved BPheo *a* bands are approximately equal and about a factor of 2 smaller than  $|\Delta\mu|$  for the special pair  $Q_y$  band; in *Rps. viridis*, the value of  $|\Delta\mu|$  for the monomer BPheo *b* band is about a factor of 3 smaller than for the special pair  $Q_y$  band. Note that the values of  $|\Delta\mu|$  for pure monomeric BPheo *a* and BPheo *b* in PMMA are of comparable magnitude (Table 1).  $|\Delta\mu|$  was estimated for the monomeric BChl bands; the value of  $|\Delta\mu|$  in *Rb. sphaeroides* ( $2.4 \pm 0.2$  D at 77 K) is slightly larger than in *Rps. viridis* (1.8

Table 1. Experimental values for the magnitude of the change in dipole moment,  $|\Delta\mu|$ , and the angle  $\zeta$ , between  $\Delta\mu$  and the transition dipole moment for the  $Q_y$  transition of the special pair in *Rps. viridis* and *Rb. sphaeroides* RCs and for pure monomeric BChls and BPheos

Chromophore	T, K	$ \Delta\mu $ , D*	$\zeta$ , °
<i>Rps. viridis</i>	298	$(10.5 \pm 0.7)/f$	$36.7 \pm 2$
special pair	77	$(6.5 \pm 0.4)/f$	$37.1 \pm 2$
<i>Rb. sphaeroides</i>	298	$(9.6 \pm 0.7)/f$	$39.5 \pm 2$
special pair	77	$(7.0 \pm 0.5)/f$	$38.1 \pm 2$
BChl <i>b</i> (6-coordinate)	77	$(2.9 \pm 0.17)/f$	$22.1 \pm 2$
BChl <i>a</i> (6-coordinate)	77	$(2.4 \pm 0.14)/f$	$11.6 \pm 2$
BPheo <i>b</i>	77	$(2.6 \pm 0.15)/f$	$23.8 \pm 2$
BPheo <i>a</i>	77	$(2.6 \pm 0.15)/f$	$9.5 \pm 2$

\*D, debye ( $3.34 \times 10^{-30}$  C·m). The value of the local field correction  $f$  may be different for each chromophore in its particular environment and at different temperatures (see text).

$\pm 0.2$  D at 77 K), whereas  $|\Delta\mu|$  is smaller for pure monomeric BChl *a* than for BChl *b* in PMMA at 77 K (Table 1).

The variations in the monomer  $Q_y$  region can be further accentuated by measuring the Stark effect spectrum as a function of the angle  $\chi$ . The spectra for each species in Fig. 5 were normalized so that the minima of the special pair  $Q_y$  Stark effect signals for the two values of  $\chi$  were equal to facilitate comparison. It is striking that normalization at this single point makes the entire special pair Stark lineshapes nearly identical as a function of  $\chi$ . The values of  $\zeta$  measured at several energies are indicated in Fig. 5, along with the difference Stark spectrum for  $\chi = 90^\circ$  minus that for  $\chi = 54.7^\circ$ . The value of  $\zeta$  measured for the monomer BPheo bands is substantially smaller than for the corresponding pure BPheo *a* or *b* (Table 1), whereas the value of  $\zeta$  measured for the monomer BChl bands is greater than for the corresponding pure BChl *a* or *b*. The difference in relative Stark enhancements and values of  $\zeta$  for each band in the monomer  $Q_y$  region presumably reflects subtle variations in the mixing of various electronic states and stands as a challenge for theoretical analysis.

**Charge-Transfer Bands.** We were especially interested to see whether there was any evidence for new bands in the Stark spectrum that do not appear in the absorption spectrum. The electronic absorption bands of pure charge-transfer transitions are likely to have small extinction coefficients and to be quite broad; however, the large value of  $|\Delta\mu|$  could enhance their detectability in the Stark spectrum. At least three charge-transfer states are of interest: ones involving charge separation within the dimer (sometimes called  $P^+P^-$ ), charge separation between the special pair and a monomeric BChl ( $P^+B^-$ ), and charge separation between the special pair and a monomeric BPheo ( $P^+H^-$ ). Estimates for the energy of the  $P^+P^-$  state range from several thousand  $\text{cm}^{-1}$  above the lowest  $\pi\pi^*$  excited state (8), to nearly degenerate with the  $\pi\pi^*$  state (17, 18). Some investigators have observed a shoulder on the red side of the special pair  $Q_y$  band, especially in *Rps. viridis* RCs (19, 20), and this shoulder has been ascribed by some to the  $P^+B^-$  charge-transfer state (20). Measurements of delayed fluorescence (21) and the temperature dependence of the  $^3P$  decay rate (22) for *Rb. sphaeroides* RCs bracket the  $P^+B^-$  state between 0.05 (21) and 0.3 eV (22) below the lowest  $\pi\pi^*$  state of the special pair at 77 K, placing the  $P^+H^-$  charge-transfer state 1–1.3 eV above the ground state. Since we are interested in estimating the energy for the vertical (Franck–Condon) transition, we must consider the displacement and shape of the potential surfaces; essentially no information is available on this point.

We have searched for new bands in the visible and near-infrared regions (340–1340 nm) of the Stark effect spectrum of *Rb. sphaeroides*. The Stark effect spectrum in the Soret region contains a number of prominent features. The individual Soret bands of the chromophores overlap significantly in the 340- to 420-nm region (the Soret band for each pigment consists of two bands,  $B_x$  and  $B_y$ ; this region is even more congested for *Rps. viridis*, which contains bound cytochrome and carotenoid). Second-derivative features are observed for each partially resolved band at about 24800, 25800, 27000, and 29000  $\text{cm}^{-1}$ ; each feature has a comparable width. It is difficult to reliably compute  $|\Delta\mu|$  for these bands because of the uncertainty in their absorption amplitudes and widths. By comparison with the appropriately weighted second derivative of the absorption spectrum (Fig. 3C) it is evident that the redmost feature at 24800  $\text{cm}^{-1}$  has the largest value of  $|\Delta\mu|$ . Using the zero-crossing points of the Stark spectrum to estimate a linewidth for the underlying transitions, we crudely estimate that  $|\Delta\mu|$  is about 2.5 D/f.  $|\Delta\mu|$  for the Soret bands of pure BChl *a* and BPheo *a* monomers (data not shown) is about 2–2.5 D/f. Although the features in the Stark effect spectrum can generally be matched with absorp-

tion features, this is not the case for the unusual band at 22800  $\text{cm}^{-1}$ . The signal is positive, suggesting that a transition at this energy gains oscillator strength in the presence of the field due to increased mixing with more intense transitions (the bump could possibly be the positive feature arising from a broad band, though there is no evidence for such a feature in the first or second derivative of the absorption).

For *Rb. sphaeroides*, the Stark effect lineshape in the region of the  $Q_x$  bands of the BPheo monomers appears as the first derivative, suggesting that the effect due to a polarizability difference dominates that due to  $|\Delta\mu|$ , as is true for pure monomeric BPheo *a* and BChl *a* (10). The Stark effect lineshape around 600 nm consists of first- and second-derivative components as well as features that cannot be accounted for by either derivative, notably the positive feature at 17700  $\text{cm}^{-1}$  and the negative feature at 16000  $\text{cm}^{-1}$ . It appears that there are several transitions in this region for which  $|\Delta\mu|$  is greater than for the  $Q_x$  bands of the BChl *a* monomers, likely including the  $Q_x$  band of the special pair.

An interesting feature in the low-temperature Stark spectrum of *Rps. viridis* is the small negative signal at  $\approx 11500$   $\text{cm}^{-1}$ , between the strong band due to the special pair and the monomeric BChl band. The corresponding absorption band is not resolved, so a quantitative analysis of  $|\Delta\mu|$  is problematic; nonetheless, we can obtain a rough estimate of about  $f^{-1}$  (3D) for this band, using the absorption at 11500  $\text{cm}^{-1}$  and assuming a linewidth of 500  $\text{cm}^{-1}$ . We also note from the data in Fig. 5 that  $\zeta$  for this band is greater than for the main special pair band. It is likely that this feature is the upper exciton component of the special pair, an assignment that is supported by other experiments (17) and some calculations (9). The corresponding region in the *Rb. sphaeroides* Stark spectrum is considerably more congested. A weak shoulder is seen on the red side of the monomeric BChl band and the positive feature on the blue side of the Stark spectrum of the special pair has an odd shape (this is best seen by comparison with the *Rps. viridis* Stark spectrum where this feature is fully resolved).

**Interpretation of Special Pair Difference Dipole.** The quantitative analysis of  $|\Delta\mu|$  and  $\zeta$  for the special pair  $Q_y$  band in *Rps. viridis* and *Rb. sphaeroides* suggests a substantial degree of charge-transfer character in the initially excited state. It is also seen that the angle between the transition dipole moment and  $|\Delta\mu|$  is quite different from that observed for pure monomeric BChls (10). Any estimate for the degree of charge transfer in the excited state based on  $|\Delta\mu|$  depends on knowledge of the ground state dipole moment. There is no experimental information on this quantity in the RC complex at the present time; we expect that the ground state dipole moment is rather small.

Scherer and Fischer (23) have presented simulations of the Stark spectrum based on a simple exciton model without the inclusion of charge-transfer states. Although this analysis purports to simulate the spectrum, this was accomplished by arbitrarily multiplying the value of  $|\Delta\mu|$  for the monomers forming the special pair by a factor of about 3, a procedure with no obvious theoretical or physical justification. We do not feel that the neglect of charge-transfer states is justified because there is substantial previous work on the absorption and electromodulation spectra of crystalline or polycrystalline polycyclic aromatics (see, e.g., refs. 24 and 25) that demonstrates unambiguously the importance of the mixing of charge-transfer states with exciton states.<sup>†</sup> Parson and Warshel (8) have stressed the importance of these charge-transfer states as determinants of the absorption maximum of

<sup>†</sup>Experiments on dimeric chlorophyll complexes that model the special pair demonstrate that  $|\Delta\mu|$  can be substantially larger for a dimer than for a monomer, suggesting that mixing with dimeric charge-transfer states can be significant (unpublished data).

the special pair  $Q_y$  bands. Although such calculations lead to specific values for  $|\Delta\mu|$  and  $\zeta$  that are comparable with what we have obtained experimentally for the special pair  $Q_y$  band (W. W. Parson, personal communication), the molecular orbitals require further refinement before quantitative comparisons are warranted.

We have never observed an electronic absorption band on the red side of the  $Q_y$  special pair band in either species, and it would likely be easily detected, if present, in the Stark effect spectrum due to the expected differences in  $|\Delta\mu|$ ,  $\zeta$ , and the linewidth. We have measured the Stark effect lineshape as a function of applied electric field strength for the  $Q_y$  transitions of *Rb. sphaeroides* in an attempt to change the relative energies of the states and the mixing between them sufficiently to produce an observable effect on the Stark effect lineshape. The predicted quadratic dependence on applied field strength (Eq. 1) was observed between  $0.74 \times 10^5$  and  $4.64 \times 10^5$  V/cm at 77 K to within 5% with no detectable change in lineshape throughout the  $Q_y$  region (data not shown). Furthermore, no change in  $\zeta$  was measured for the special pair  $Q_y$  band over this range of applied field strength. Thus, there is no evidence for spectral changes in the Stark spectrum induced by a change in the energy of or coupling to other states.

The value of  $f|\Delta\mu|$  for the  $Q_y$  transition of the special pair in both species decreases substantially when the temperature is decreased, while that for the other bands decreases considerably less. The value of  $f|\Delta\mu|$  for BPheo *a* in PMMA was temperature independent within the experimental uncertainty, while the value of  $f|\Delta\mu|$  for a chlorophyll derivative in apomyoglobin embedded in PVA decreased by about 20% between room temperature and 77 K (unpublished data). The low-frequency dielectric constant of PVA decreases by about a factor of 2 between room temperature and 77 K (26). Since the local field correction  $f$  depends on the dielectric constant of the matrix, the observed value of  $f|\Delta\mu|$  will also be temperature dependent. The exact form of the dependence of  $f$  on the dielectric constant is highly sensitive to the method used to model the dielectric environment of the chromophore; however, at least part of the difference in  $f|\Delta\mu|$  for the special pair as a function of temperature can be accounted for by the change in dielectric constant. The change in  $f|\Delta\mu|$  with temperature for the model chlorophyll in apomyoglobin system is comparable with the change observed for the monomer bands in the RC. The variation with temperature for the special pair  $Q_y$  bands is considerably larger, and it may reflect more subtle local variations in the dielectric or electronic properties of this component.

We are very much indebted to Prof. W. W. Parson and Dr. D. Middendorf for providing the samples of *Rps. viridis* RCs used in these experiments and for extensive and helpful discussions. We also acknowledge helpful discussions with Prof. M. Okamura and Drs. M. Lösche and R. Goldstein. We thank Profs. W. W. Parson, P.

Petelenz, and B. Honig for making manuscripts available prior to publication. The germanium detector was borrowed from the ADC Corp. (Fresno, CA). This work was supported by grants from the National Science Foundation and the Gas Research Institute. S.G.B. is the recipient of a Presidential Young Investigator Award.

1. Deisenhofer, J., Epp, O., Miki, K., Huber, R. & Michel, H. (1984) *J. Mol. Biol.* **180**, 385–398.
2. Deisenhofer, J., Epp, O., Miki, K., Huber, R. & Michel, H. (1985) *Nature (London)* **318**, 618–624.
3. Allen, J. P., Feher, G., Yeates, T. O., Rees, D. C., Deisenhofer, J., Michel, H. & Huber, R. (1986) *Proc. Natl. Acad. Sci. USA* **83**, 8589–8593.
4. Chang, C. H., Tiede, D., Tang, J., Smith, U., Norris, J. & Schiffer, M. (1986) *FEBS Lett.* **205**, 82–86.
5. Parson, W. W., Scherz, A. & Warshel, A. (1985) *Springer Ser. Chem. Phys.* **42**, 122–130.
6. Knapp, E. W., Fischer, S. F., Zinth, W., Sander, M., Kaiser, W., Deisenhofer, J. & Michel, H. (1985) *Proc. Natl. Acad. Sci. USA* **82**, 8463–8467.
7. Knapp, E. W., Scherer, P. O. J. & Fischer, S. F. (1986) *Biochim. Biophys. Acta* **852**, 295–305.
8. Parson, W. W. & Warshel, A. (1987) *J. Am. Chem. Soc.* **109**, 6152–6163.
9. Eccles, J. & Honig, B. (1988) *Biophys. J.*, in press.
10. Lockhart, D. J. & Boxer, S. G. (1987) *Biochemistry* **26**, 664–668, and correction (1987) **26**, 2958.
11. deLeeuw, D., Malley, M., Butterman, G., Okamura, M. Y. & Feher, G. (1982) *Biophys. Soc. Abstr.* **37**, 111a.
12. Boxer, S. G., Lockhart, D. J. & Middendorf, T. R. (1987) in *Primary Processes in Photobiology*, ed. Kobayashi, T. (Springer, New York), in press.
13. Schenck, C. C., Blankenship, R. E. & Parson, W. W. (1982) *Biochim. Biophys. Acta* **680**, 44–49.
14. Scherz, A. & Parson, W. W. (1984) *Biochim. Biophys. Acta* **766**, 653–665.
15. Liptay, W. (1974) in *Excited States*, ed. Lim, E. C. (Academic, New York), Vol. 1, pp. 129–229.
16. Mathies, R. & Stryer, L. (1976) *Proc. Natl. Acad. Sci. USA* **73**, 2169–2173.
17. Meech, S. R., Hoff, A. J. & Wiersma, D. A. (1986) *Proc. Natl. Acad. Sci. USA* **83**, 9464–9468.
18. Won, Y. & Friesner, R. A. (1987) *Proc. Natl. Acad. Sci. USA* **84**, 5511–5515.
19. Vermeglio, A. & Paillotin, G. (1982) *Biochim. Biophys. Acta* **681**, 32–40.
20. Shuvalov, V. A. & Klevanik, A. V. (1983) *FEBS Lett.* **160**, 51–55.
21. Woodbury, N. W. T. & Parson, W. W. (1981) *Biochim. Biophys. Acta* **767**, 345–361.
22. Chidsey, C. E. D., Takiff, L., Goldstein, R. A. & Boxer, S. G. (1985) *Proc. Natl. Acad. Sci. USA* **82**, 6850–6854.
23. Scherer, P. O. J. & Fischer, S. F. (1986) *Chem. Phys. Letts.* **131**, 153–159.
24. Sebastian, L., Weiser, G., Peter, G. & Bässler, H. (1983) *Chem. Phys.* **75**, 103–114.
25. Munn, R. W., Petelenz, P. & Siebrand, W. (1987) *Chem. Phys.* **111**, 209–221.
26. Ishida, Y., Takada, Y. & Takayanagi, M. (1960) *Kolloid-Z.* **168**, 121–124.